Th G105 11

A Frequency-domain Seismic Modeling Engine for 3D Visco-acoustic VTI Full Waveform Inversion of Fixed-spread Data

S. Operto (CNRS - University of Nice Sophia-Antipolis), R. Brossier* (University of Grenoble), L. Combe (University of Grenoble), L. Métivier (CNRS - University of Grenoble), A. Ribodetti (IRD - University of Nice Sophia-Antipolis) & J. Virieux (University of Grenoble)

SUMMARY

Frequency-domain full waveform inversion (FWI) of fixed-spread data can be limited to a few discrete frequencies thanks to the redundant control of frequency and scattering angle on the wavenumber coverage. In this framework, 3D finite-difference frequency-domain seismic modeling can be efficiently performed for multiple sources in the visco-acoustic approximation with sparse direct solver. We extend the so-called mixed-grid finite-difference stencil to account for vertical transverse isotropy in visco-acoustic frequency-domain seismic modeling without extra computational cost. The VTI acoustic wave equation is recast as a fourth-order wave equation, which can be decomposed into an elliptic wave equation and an anelliptic term. The discretization of this equation only requires a straightforward adaptation of the existing isotropic stencil. A discretization rule of 4 grid points per minimum wavelength, which is suitable for FWI applications, is used for frequency-domain seismic modeling. We validate our finite-difference frequency-domain method against a finite-difference time-domain method using a smooth VTI acoustic model of the Valhall oil field. Comparison between the real and modeled data for the 7-Hz frequency suggests that our method can provide a suitable modeling engine to perform multi-parameter FWI of fixed-spread data in visco-acoustic VTI media.

Introduction

Frequency-domain full waveform inversion (FWI) of fixed-spread data can be limited to a few discrete frequencies (e.g. Pratt, 1999). In this framework, frequency-domain modeling can be efficiently performed for multiple sources by solving the time-harmonic wave equation with sparse direct solvers: a lower-upper (LU) decomposition of the so-called impedance matrix is performed before computing the solutions by substitutions. Although the LU decomposition is expensive, Operto et al. (2007) and many others since then have shown the feasibility of 3D DSFDM at low frequencies. Recent developments that take advantage of some low-rank properties of the impedance matrix have further improved the efficiency of 3D DSFDM (Wang et al., 2012; Weisbecker et al., 2013).

The LU factorization requires designing finite-difference stencil with specifications that differ from those used in finite-difference time-domain (FDTD) modeling (Operto et al., 2007): both the dimension and the numerical bandwidth of the matrix must be minimized. The first requirement direct us toward 2nd-order wave equation through a parsimonious approach. Moreover, the stencil should provide a sufficient accuracy for a discretization rule of four grid points per wavelength, which is consistent with the theoretical resolution of FWI. This prevents using 2nd-order accurate stencil. On the other hand, minimization of the numerical bandwidth prevents using high-order accurate stencil. The so-called mixed grid approach (Jo et al., 1996) aims to conciliate these apparently contradictory requirements with two recipes: the first one linearly combines several stiffness matrices that are built on different rotated coordinate systems to mitigate numerical anisotropy. The second one spreads the mass term over the nodes involved in the stencil to minimize numerical dispersion. The resulting stencil has the same numerical bandwidth than a 2nd-order accurate stencil and a similar or even better accuracy than a 4th-order accurate stencil.

The 3D visco-acoustic (isotropic) DSFDM stencil is presented in Operto et al. (2007) and Brossier et al. (2010). Here, we extend this stencil to introduce vertical transverse isotropy (VTI) in 3D visco-acoustic modeling, as it is often mandatory to account for anisotropy in FWI. Following Wang et al. (2012), we recast the visco-acoustic VTI wave equation as a 4th-order partial differential equation, starting from the velocity-stress elastodynamic wave equation for VTI media and canceling the shear wavespeed on the symmetry axis (Duveneck and Bakker, 2011). We show how this equation can be easily implemented after a slight adaptation of the isotropic 27-point mixed-grid stencil. Numerical simulation in a realistic VTI model from the Valhall oil field illustrates the potential of the method as a modeling engine for visco-acoustic VTI FWI of ocean-bottom seismic data.

Fourth-order acoustic VTI equation

A frequency-domain VTI acoustic wave equation can be recast as a system of 2nd-order partial differential equations if the shear wavespeed on the symmetry axis is set to zero in the first-order velocity-stress elastodynamic equations followed by the elimination of the particle velocity wavefields:

$$\frac{\omega^2}{\kappa_0} g \quad + \quad (1+2\varepsilon)(\mathscr{X}+\mathscr{Y})\, g + \sqrt{1+2\delta}\,\mathscr{Z}\, q = \frac{\omega^2 s_g}{\kappa_0} s, \tag{1}$$

$$\frac{\omega^2}{\kappa_0} q \quad + \quad \sqrt{1+2\delta}\,(\mathscr{X}+\mathscr{Y})\, g + \mathscr{Z}\, q = \frac{\omega^2 s_q}{\kappa_0} s. \tag{2}$$

where $\kappa_0 = \rho V_{P0}^2$, ρ is the density, V_{P0} is the vertical wavespeed, δ and ε are the Thomsen's parameters. The pressure wavefield p is given by $(1/3)(2g+q)$. In equations 1-2, we introduce the following notations for the 2nd-order differential operators:

$$\mathscr{X} = \frac{1}{\xi_x}\partial_x \frac{b}{\xi_x}\partial_x, \quad \mathscr{Y} = \frac{1}{\xi_y}\partial_y \frac{b}{\xi_y}\partial_y, \quad \mathscr{Z} = \frac{1}{\xi_z}\partial_z \frac{b}{\xi_z}\partial_z.$$

where b is the buoyancy, the inverse of density, $b = 1/\rho$. We introduce perfectly-matched layer (PML) absorbing conditions through the 1D functions $\xi_x = 1 + i\frac{\gamma_x}{\omega}$, $\xi_y = 1 + i\frac{\gamma_y}{\omega}$ and $\xi_z = 1 + i\frac{\gamma_z}{\omega}$, where functions

γ_x, γ_y and γ_z control the damping of the wavefield in the PMLs (Operto et al., 2007). The source excitation in the frequency domain is denoted by s and we found $s_g = \frac{2(1+2\varepsilon)+\sqrt{1+2\delta}}{D}$ and $s_q = \frac{1+2\sqrt{1+2\delta}}{D}$ with $D = 4\sqrt{1+2\varepsilon}+4\sqrt{1+2\delta}+1$ for explosive source.

We aim to eliminate q from equations 1-2 to derive a 4th-order equation for g. We found

$$q = \frac{1}{\sqrt{1+2\delta}}\,g + \frac{2(\varepsilon-\delta)\kappa_0}{\omega^2\sqrt{1+2\delta}}\,(\mathscr{X}+\mathscr{Y})\,g + \left(s_q - \frac{1}{\sqrt{1+2\delta}}\,s_g\right)s. \tag{3}$$

Injecting the expression of q in equation 1 gives the 4th-order equation satisfied by g:

$$\omega^2\left[\frac{\omega^2}{\kappa_0}+(1+2\varepsilon)\,(\mathscr{X}+\mathscr{Y})+\sqrt{1+2\delta}\,\mathscr{Z}\frac{1}{\sqrt{1+2\delta}}\right]g + 2\sqrt{1+2\delta}\,\mathscr{Z}\frac{\kappa_0(\varepsilon-\delta)}{\sqrt{1+2\delta}}\,(\mathscr{X}+\mathscr{Y})\,g$$
$$= \frac{\omega^4 s_g}{\kappa_0}\,s - \omega^2\sqrt{1+2\delta}\,\mathscr{Z}\left(s_q - \frac{1}{\sqrt{1+2\delta}}\,s_g\right)s. \tag{4}$$

For homogeneous δ, equation 4 shows that the VTI equation can be decomposed into an elliptic anisotropic operator $(\frac{\omega^2}{\kappa_0}+(1+2\varepsilon)\,(\mathscr{X}+\mathscr{Y})+\mathscr{Z})$ and an anellipticity term $(2\,\mathscr{Z}\,\kappa_0(\varepsilon-\delta)\,(\mathscr{X}+\mathscr{Y}))$.

Finite-difference discretization

The VTI acoustic equation, eq. 4, is implemented after a slight adaptation of the isotropic stencil (Operto et al., 2007). The isotropic and VTI wave equations can be written in compact form as:

$$Isotropic:\ [\mathbf{M}+\mathbf{S}]\,\mathbf{p}=\mathbf{s};\ \ VTI:\ \omega^2\{[\mathbf{M}_e+\mathbf{S}_e]\,\mathbf{g}\}+\mathbf{E}\,\mathbf{g}=\mathbf{s}',\ \mathbf{q}=\mathbf{B}\,\mathbf{g}+\mathbf{s}",\ \mathbf{p}=(1/3)(2\,\mathbf{g}+\mathbf{q}).$$

The mass matrix $\mathbf{M}_e$ is built with the same anti-lumped mass strategy than the isotropic counterpart $\mathbf{M}$.

The elliptic stiffness matrix $\mathbf{S}_e$ is easily inferred from the isotropic counterpart $\mathbf{S}$. First, we multiply each coefficient of $\mathbf{S}$ that involves an horizontal spatial derivative with $(1+2\varepsilon_k)$ where k is the index of the row to which the coefficient belongs. Second, we need to form the matrix-vector product $\sqrt{1+2\delta}\,\mathscr{Z}(g/\sqrt{1+2\delta})$. We first discretize $\sqrt{1+2\delta}\,\mathscr{Z}$ by multiplying each coefficient of $\mathbf{S}$ that involves a vertical spatial derivative with $\sqrt{1+2\delta_k}$, where k is the index of the row to which the coefficient belongs. Then, we inject the discrete expressions of $g/\sqrt{1+2\delta}$ in the matrix-vector product, that amounts to divide each coefficient that involves a vertical spatial derivative in $\mathbf{S}$ by $\sqrt{1+2\delta_l}$, where l is the column index to which the coefficient belongs.

The anelliptic matrix $\mathbf{E}$ is discretized with a parsimonious 2nd-order accurate staggered-grid stencil, which preserves the spatial support of the stencil over two grid intervals. Once $\mathbf{g}$ is computed, we infer $\mathbf{q}$ from eq. 3. We discretize the matrix $\mathbf{B}$ with a 2nd-order accurate stencil, although any other stencil can be used as computation of q does not require system resolution.

VTI modeling is performed at the same cost than isotropic modeling. A dispersion analysis in homogeneous media shows that the weighting coefficients of the mixed-grid stencil that were obtained for the isotropic equation can be re-used for modeling in elliptic media with the same discretization rule of 4 grid points per wavelength. These coefficients were found quite insensitive to the value of ε.

Numerical examples

We validate the DSFDM method against a $\mathscr{O}(\Delta t^2,\Delta x^4)$ staggered-grid finite-difference time-domain (FDTD) method. We use the sparse direct solver MUMPS (Amestoy et al., 2000) to perform the LU factorization, which was computed in single and double precision without differences in the results. The fill-reducing matrix ordering is performed with a nested-dissection algorithm. We observed some instabilities in the PMLs for VTI media, when the grid interval is significantly smaller that a quarter of a wavelength. Pragmatically, we force the medium to be elliptic in the PMLs to avoid these instabilities.

We present some simulations in a VTI visco-acoustic model of the Valhall oil field (Fig. 1(a-b)) that was developed by reflection traveltime tomography (courtesy of BP). The water depth is around 70m. The subsurface is characterized by soft sediments above low-velocity gas layers. The reservoir at 2.5 km in depth delineates a sharp positive velocity contrast. The maximum anisotropy reaches a value of 15 percent. The model dimensions are 16km x 9km x 4.5km.

We compare VTI monochromatic wavefields computed with DSFDM and FDTD for the 7-Hz frequency and a source located on the sea bottom at (x=3.1km,y=13km,z=0.07km). The grid intervals are 50m and 25 m for DSFDM and FDTD, respectively. This gives a discretization of 4 grid points per minimum wavelength in DSFDM. The grid dimensions are 182 x 322 x 92 for DSFDM. Adding eight grid points in the PMLs leads to 6.7 millions of unknowns. A free surface condition is set on top of the model. The source is positioned in the finite-difference grid with a sinc parameterization (Hicks, 2002). The length of the FDTD simulation is 20s and guarantees that the steady-state regime is reached. DSFDM was performed on four quadri-processor AMD Opteron nodes with 384Gb of shared memory per node with Infiniband network. We use 16 Message-Passing-Interface (MPI) processes distributed over four nodes and four threads per MPI process for linear algebra tasks performed with the Basic Linear Algebra Subroutines (BLAS3). The LU factorization and the substitution per source took 42mn and 1.4 s, respectively. The agreement between DSFDM and FDTD wavefields can be qualitatively assessed in Figure 1(c-d)). Comparison between real data and DSFDM solutions extracted at 5m in depth below the sea surface shows a good agreement owing to the fact that the smooth Valhall model does not predict the full wavefield complexity (Fig. 2). In particular, we notice some mismatches at offsets where reflected waves and low-velocity layers have a significant footprint in the monochromatic wavefield.

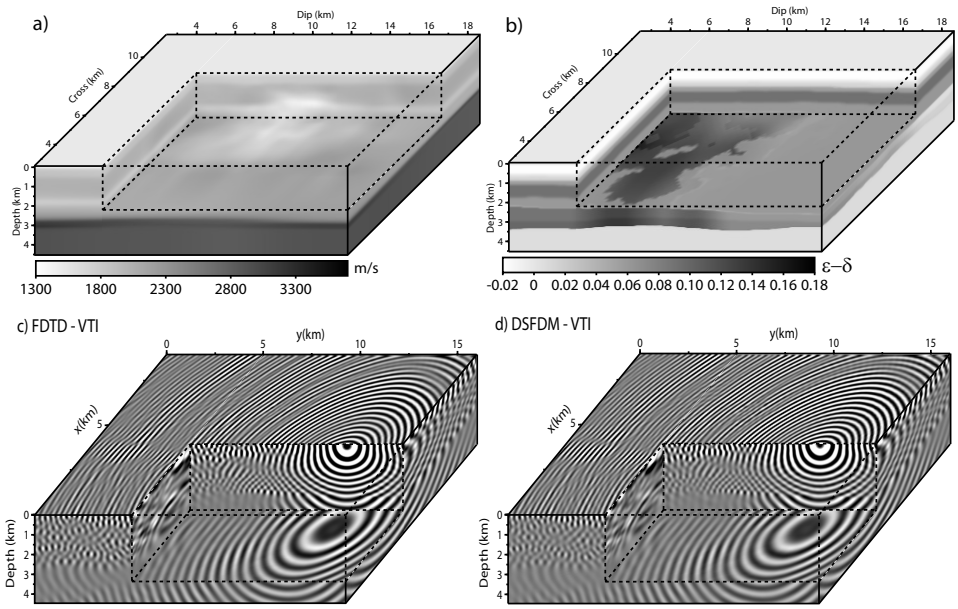

Figure 1 *(a-b) Valhall model. (a)* V_{P0}*. (b)* $\varepsilon - \delta$*. (c-d) Seven-Hz wavefield. (c) FDTD. (d) DSFDM.*

Conclusion

We have presented a parsimonious finite-difference frequency-domain method that is suitable to perform visco-acoustic modeling in vertical transversely isotropic media with sparse direct solver. This modeling engine is designed for FWI of fixed-spread data in which anisotropic and attenuation effects can be introduced. A discretization rule of four grid points per wavelength is enough to guarantee accurate simulations and is consistent with the theoretical resolution of FWI. The implementation of the block low-rank approximation in sparse direct solver should still increase the computational efficiency of the method. An open question remains the efficient extension in TTI media.

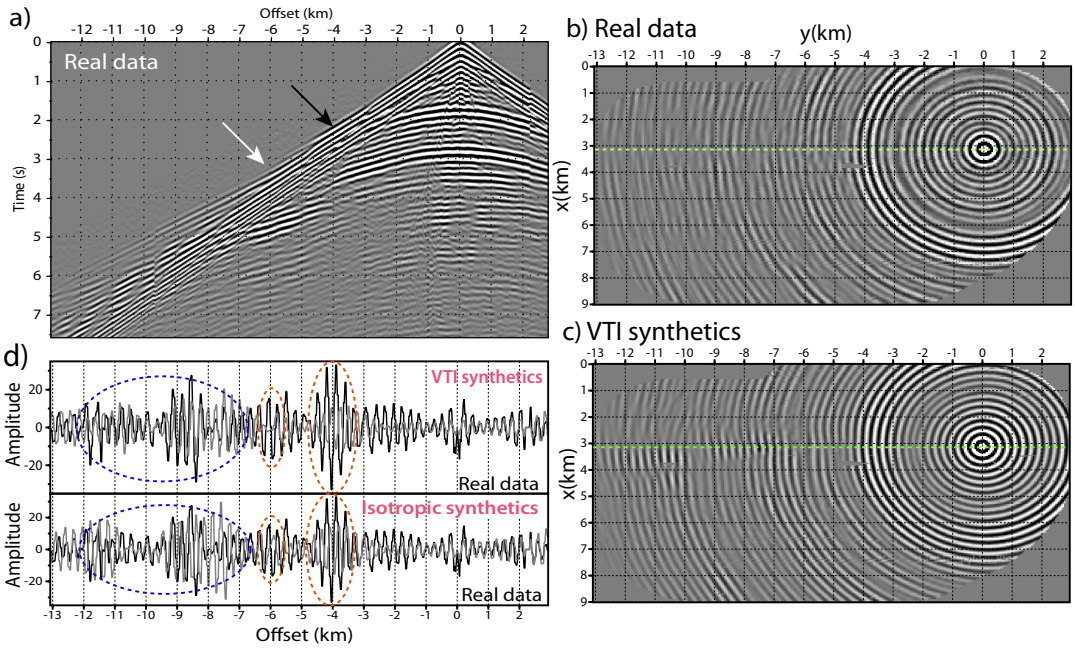

Figure 2 *Valhall. (a) Real receiver gather. Black and white arrows point a subcritical reflection and a polarity reversal in the first arrival, respectively. (b-c) Real data (b) and DSFDM data (c) for the 7-Hz frequency. DSFDM data were multiplied with the source signature that was estimated by matching the real data with the DSFDM Green functions. (d) Comparison along the yellow line in (b-c) between real data (black) and VTI/isotropic (top/bottom) DSFDM data (gray), plotted with an amplitude gain with offset. Mismatches (red ellipses) are shown at offsets where the Valhall model does not predict the wavefield complexity (arrows in (a)). VTI synthetics match better the real data than isotropic ones at long offsets where anisotropic effects are significant (blue ellipse).*

Acknowledgments

This study was funded by the SEISCOPE II consortium (*http://seiscope2.osug.fr*). This study was granted access to the HPC facilities of SIGAM (Observatoire de la Cote d'Azur).

References

Amestoy, P., Duff, I.S. and L'Excellent, J.Y. [2000] Multifrontal parallel distributed symmetric and unsymmetric solvers. *Computer Methods in Applied Mechanics and Engineering*, **184**(2-4), 501–520.

Brossier, R., Etienne, V., Operto, S. and Virieux, J. [2010] Frequency-domain numerical modelling of visco-acoustic waves based on finite-difference and finite-element discontinuous galerkin methods. In: Dissanayake, D.W. (Ed.) *Acoustic Waves*. SCIYO, ISBN 978-953-307-111-4, 125–158.

Duveneck, E. and Bakker, P.M. [2011] Stable P-wave modeling for reverse-time migration in tilted TI media. *Geophysics*, **76**(2), S65–S75.

Hicks, G.J. [2002] Arbitrary source and receiver positioning in finite-difference schemes using kaiser windowed sinc functions. *Geophysics*, **67**, 156–166.

Jo, C.H., Shin, C. and Suh, J.H. [1996] An optimal 9-point, finite-difference, frequency-space 2D scalar extrapolator. *Geophysics*, **61**, 529–537.

Operto, S., Virieux, J., Amestoy, P., L'Éxcellent, J.Y., Giraud, L. and Ben Hadj Ali, H. [2007] 3D finite-difference frequency-domain modeling of visco-acoustic wave propagation using a massively parallel direct solver: A feasibility study. *Geophysics*, **72**(5), SM195–SM211.

Pratt, R.G. [1999] Seismic waveform inversion in the frequency domain, part I : theory and verification in a physic scale model. *Geophysics*, **64**, 888–901.

Wang, S., Xia, J., de Hoop, M.V. and Li, X.S. [2012] Massively parallel structured direct solver for equations describing time-harmonic qP-polarized waves in TTI media. *Geophysics*, **77**(3), T69 – T82.

Weisbecker, C. et al. [2013] 3D frequency-domain seismic modeling with a block low-rank algebraic multifrontal direct solver. *SEG Technical Program Expanded Abstracts 2007*.